TISSUE ENGINEERING: Part A
Volume 16, Number 3, 2010

DOI: 10.1089/ten.tea.2009.0439

In Vitro and *In Vivo* Osteogenesis of Porcine Skin-Derived Mesenchymal Stem Cell–like Cells with a Demineralized Bone and Fibrin Glue Scaffold

Eun-Ju Kang, D.V.M.,[1] June-Ho Byun, D.D.S., Ph.D.,[2] Young-Jin Choi, D.D.S.,[2] Geun-Ho Maeng, D.V.M.,[1] Sung-Lim Lee, D.V.M., Ph.D.,[1] Dong-Ho Kang, M.D.,[3] Jong-Sil Lee, M.D., Ph.D.,[4] Gyu-Jin Rho, D.V.M., Ph.D.,[1] and Bong-Wook Park, D.D.S., Ph.D.[2]

In vitro and *in vivo* osteogenesis of skin-derived mesenchymal stem cell–like cells (SDMSCs) with a demineralized bone (DMB) and fibrin glue scaffold were compared. SDMSCs isolated from the ears of adult miniature pigs were evaluated for the expression of transcriptional factors (Oct-4, Sox-2, and Nanog) and MSC marker proteins (CD29, CD44, CD90, and vimentin). The isolated SDMSCs were cocultured *in vitro* with a mixed DMB and fibrin glue scaffold in a nonosteogenic medium for 1, 2, and 4 weeks. Osteonectin, osteocalcin, and Runx2 were expressed during the culture period and reached maximum at 2 weeks after *in vitro* coculture. von Kossa–positive bone minerals were also noted in the cocultured medium at 4 weeks. Autogenous porcine SDMSCs (1×10^7) labeled with a tracking dye, PKH26, were grafted into the maxillary sinus with a DMB and fibrin glue scaffold. In the contralateral side, only a scaffold was grafted without SDMSCs (control). *In vivo* osteogenesis was evaluated from two animals euthanized at 2 and 4 weeks after grafting. *In vivo* PKH26 staining was detected in all the specimens at both time points. Trabecular bone formation and osteocalcin expression were more pronounced around the grafted materials in the SDMSC-grafted group compared with the control group. New bone generation was initiated from the periphery to the center of the grafted material. The number of proliferating cells increased over time and reached a peak at 4 weeks in both *in vivo* and *in vitro* specimens. These findings suggest that autogenous SDMSC grafting with a DMB and fibrin glue scaffold can serve as a predictable alternative to bone grafting in the maxillary sinus floor.

Introduction

Pneumatization of the maxillary sinus and atrophy of the alveolar ridge can disturb implant placement in the maxillary posterior alveolar ridge. In such cases, various bone grafting techniques are needed for successful dental implant placement. Autogenous bone grafting has been the gold standard, but donor site morbidity, limited volume, and difficulty in shaping limit this approach.[1,2] Allogenic bone and allomaterial are good substitutes for autogenous bone, but the extended time to bone consolidation after grafting of these materials, and the potential for an immune reaction or poor bone quality, must be considered.[3]

Recently, tissue-engineered bones have been used in the maxillofacial regions as an alternative to various other bone graft materials. Tissue-engineered bone derived from autogenic sources may eliminate the problems of donor site morbidity associated with autogenic grafts, the immunogenicity associated with allogenic grafts, and the potential loosening associated with alloplastic materials.[4,5] However, primitive pluripotent or multipotent cells are essential for tissue-engineered bone formation. Several literatures show that bone marrow mesenchymal stem cells (MSCs),[5–8] periosteum-derived precursor cells,[1,9–11] and autologous bone-derived cells[2,12] have been the main sources of tissue-engineered bone. Nevertheless, harvesting of these primary tissues for use in tissue engineering may require another invasive technique and may lead to various complications, such as hematoma formation, bleeding, infection, and substantial pain.

There are many potential sources of adult stem cells for regenerative medicine, such as bone marrow, umbilical cord blood, fat tissues, circulating blood cells, dental tissues, and skin. Skin is the tissue that has most recently been considered as an adult stem-cell source and is highly accessible and easily obtained autogenous tissue with minimal donor site complications.[13] Moreover, skin is an abundant pluripotent and

[1]College of Veterinary Medicine, Gyeongsang National University, Jinju, Republic of Korea.
[2]Department of Oral & Maxillofacial Surgery, School of Medicine and Institute of Health Sciences, Gyeongsang National University, Jinju, Republic of Korea.
Departments of [3]Neurosurgery and [4]Pathology, School of Medicine, Gyeongsang National University, Jinju, Republic of Korea.

multipotent cell source that has immune privilege and the potential for self-replication.[14] Several studies have shown that there are many different types of stem cells, such as epidermal stem cells, MSC-like cells, and skin-derived progenitors, in the hair follicle, bulge, and epidermis of the skin.[14–17] Among them, the skin-derived precursor cells (SKPs) were most actively studied in regenerative medicine.

SKPs were originated from dermis and appeared as floating spheres in the culture condition in the presence of the fibroblast growth factor-2 (FGF2) and epidermal growth factor (EGF).[18–21] Moreover, SKPs had distinct characteristics from MSCs, and SKPs had represented the characteristics of embryonic neural crest-derived precursor cells that persist in adulthood.[20–24] These results suggest that SKPs may have many benefits in the regeneration of nervous system.[25,26] Excepting these neurogenic SKPs, many kinds of stem cells are present in the skin and its appendages, including MSC, epidermal stem cell, hematopoietic stem cell, and melanocyte stem cell.[14] These skin stem cells may have multipotency and they can be used in the regenerative medicine. In this study, we focused on the *in vivo* osteogenesis of these skin-derived stem cells, so we isolated skin-derived MSC-like cells (SDMSCs) with nonfloating cell culture methods from adult porcine ear skin. Previously we have demonstrated that these skin-derived cells possess *in vitro* osteogenic, adipogenic, and neurogenic differentiation potential.[27]

This study was therefore conducted to characterize porcine SDMSCs (pSDMSCs) by evaluating the expressions of various MSC markers (CD29, CD44, CD90, and vimentin) and transcription factors (Oct-4, Sox-2, and Nanog). Further, the *in vivo* osteogenesis of autogenous pSDMSCs after grafting into the maxillary sinus floor with a demineralized bone (DMB) and fibrin glue scaffold, was evaluated. In addition, *in vitro* osteogenesis of pSDMSCs cocultured with a DMB and fibrin glue scaffold was also assessed.

Materials and Methods

Isolation and culture of pSDMSCs

Four miniature pigs, aged 6 months to 1 year and weighing approximately 25 kg, were used in this study. All experiments were authorized by the Animal Center for Medical Experimentation at the Gyeongsang National University.

Animals were sedated with an intramuscular injection of 4 mg/kg of azaperone (Stresnil®; Janssen Animal Health for Merial Canada Inc., Baie d'Urfe, Quebec, Canada) before general anesthesia. General anesthesia was induced with an intravenous injection of 10 mg/kg of tiletamine–zolazepam (Zoletil®; Virbac, Carros, France). Under aseptic conditions, ear skin samples of full thickness were obtained and sliced into 1–2 mm^2 explants containing epidermis and dermis, as well as all skin appendages like hair follicles, sebaceous glands, and sweat glands. Skin explants were cultured in 2 mL of Dulbecco's modified Eagle's medium (DMEM)/F12 (1:1) (Invitrogen, Carlsbad, CA) supplemented with 10% fetal bovine serum (FBS; Invitrogen), 10 ng/mL EGF (Sigma-Aldrich, St. Louis, MO), 10 ng/mL FGF2 (Sigma-Aldrich), 100 U/mL penicillin (Sigma-Aldrich), and 100 μg/mL streptomycin (Sigma-Aldrich) in 35 mm dishes (Nunc, Roskilde, Denmark) at 38.5°C in a humidified atmosphere of 5% CO_2 in air for 2 days. After removal of the remaining skin fragments, the attached cells were expanded *in vitro* with change of culture medium twice a week. Once confluent, cells were dissociated using 0.25% (w/v) trypsin–ethylenediaminetetraacetic acid (EDTA; Invitrogen) solution and pelleted at 500 *g* for 5 min. Cells were then regrown and allowed for five passages.

Cell surface and intracellular marker analysis

Cell surface and intracellular markers of pSDMSCs at fifth passage were analyzed by flow cytometer (BD FACSCalibur; Becton Dickinson and Company, Franklin Lakes, NJ) in three replicates. In brief, cells that reached 90% confluence were harvested using 0.25% EDTA and washed twice in Dulbecco's phosphate-buffered saline (DPBS; Invitrogen) supplemented with 10% FBS. To detect CD44 and CD90, cells were directly labeled with fluorescein isothiocyanate–conjugated CD markers (CD44 [1:100; BD Pharmingen™, BD Biosciences, Franklin Lakes, NJ] and CD90 [1:100; BD Pharmigen]). To analyze, CD29 and vimentin, cells were fixed in 3.7% formaldehyde for 1 h. After being washed with DPBS, samples were labeled with primary antibodies (CD29 [1:100; BD Pharmigen] and vimentin [1:100; Sigma-Aldrich]) for 1 h and subsequently labeled with secondary antibody (1:100; BD Pharmigen).

In vitro *coculture of pSDMSCs with a DMB and fibrin glue scaffold*

A total of 7×10^5 SDMSCs mixed with fibrin glue (Greenplast® kit, Green Cross, Yongin, Korea) was injected into a DMB (Grafton®, Osteotech™, Eatontown, NJ) scaffold. The scaffold was incubated in DMEM supplemented with 10% FBS at 38.5°C in a humidified atmosphere of 5% CO_2 in air, with culture medium changed twice a week. At 4 weeks of incubation, the scaffold was evaluated for *in vitro* osteogenesis using von Kossa staining, as previously described.[9]

After 1, 2, and 4 weeks of incubation, the scaffold was rinsed with DPBS and fixed in 3.7% (w/v) formaldehyde solution, and differentiated cells were isolated using cell stainer (BD Falcon™, BD Biosciences, Franklin Lakes, NJ) for total RNA. The fixed scaffold was embedded with paraffin for histological evaluation. The paraffin blocks were cut into 4 μm sections, stained with hematoxylin and eosin after being deparaffinized, and hydrated. The specimens were photographed under microscopy, and the observed cells were counted and calculated per cm^2. A minimum of three sections were evaluated per culture plate at each time point for *in vitro* coculture cell counting.

Reverse transcription–polymerase chain reaction analysis

At passages 2 and 5, pSDMSCs were evaluated for the expressions of transcription factors, such as Oct-4, Sox-2, and Nanog. In addition, the relative abundance of osteonectin, osteocalcin, and Runx2 as bone-related glycoproteins and osteoblast marker of pSDMSCs cultured in the scaffold was analyzed using reverse transcription–polymerase chain reaction (RT-PCR). Primers of transcription factors were designed as previously described.[28] RT-PCR primers for markers of transcription factors and bone-related glycoproteins are summarized in Table 1. Total RNA was extracted from cultured cells using an RNeasy Mini Kit (Qiagen, Valencia, CA). cDNA synthesis was performed for 30 min at 55°C using an Omniscript Reverse Transcription Kit (Qiagen) with oligo-dT

Table 1. Reverse Transcription–Polymerase Chain Reaction Primers Used for Evaluating Transcription Factors and Osteogenic Differentiation

Gene	*Sequence of primer (5′–3′)*	*Amplification size*	*Temperature (°C)*
GAPDH	F-GGGCATGAACCATGAGAAGT R-AAGCAGGGATGATGTTCTGG	230	60
OCT-4	F-AGGTGTTCAGCCAAACGACC R-TGATCGTTTGCCCTTCTGGC	335	60
Nanog	F-ATCCAGCTTGTCCCCAAAG R-ATTTCATTCGCTGGTTCTGG	438	60
Sox-2	F-GCCTGGGCGCCGAGTGGA R-GGGCGAGCCGTTCATGTAGGTCTG	443	64
Osteonectin	F-TCCGGATCTTTCCTTTGGTTTCTA R-CCT TCA CAT CGT GGC AAG AGT TTG	187	58
Osteocalcin	F-CTGGACCAACATCTTGAGCA R-ACCCCTTTGGTGGTGTTGTA	205	58
Runx2	F-CAGACCAGCAGCACTCCATA R-AACGCCATCGTTCTGGTTAG	171	58

GAPDH, glyceraldehyde-3-phosphate dehydrogenase.

primers. The cDNAs produced were used as a template for PCR amplification. PCR was performed using Maxime PCR Premix (iNtRON Biotechnology, Sungnam, Korea): 3 min denaturation at 94°C, followed by 34 cycles at 94°C for 45 s, annealing for 30 s, elongation at 72°C for 45 s (transcription factor) and 90 s (bone-related genes), and a final extension at 72°C for 10 min using Thermocycler (PTC-200, GMI™, Anoka, MN).

Quantitative PCR for the detection of osteonectin and osteocalcin of the pSDMSCs in the scaffold was performed using LightCycler® Faststart DNA Master SYBR Green dye (Roche, Pleasanton, CA) in a 20 μL reaction volume: 10 min denaturation at 95°C, followed by 45 cycles at 95°C for 10 s, annealing for 10 s, and elongation at 72°C for 15 s using LightCycler (Roche). The mean value of the six measurements was used for statistical analysis.

Cell membrane fluorescent labeling

Once pSDMSCs reached nearly 70% confluence, cell membrane labeling was performed using PKH26 Red Fluorescent Cell Linker Kit (Sigma-Aldrich®, St. Louis, MO), as per the manufacturer's instructions. Briefly, cells were harvested using trypsin/EDTA and washed in Ca^{+}- and Mg^{+}-free DPBS by centrifugation at 400 *g* for 5 min. After adjusting the cell concentration to 1×10^{7} cells, 1 mL of diluent C and 1 mL of 4×10^{-6} M PKH26 dye were added. The sample was then mixed and incubated at 25°C for 5 min. The reaction was stopped by adding 2 mL of 10% FBS for 1 min. Finally, the stained cells were washed three times with DMEM/F12 medium.

Maxillary sinus floor elevation using autogenous pSDMSCs with a DMB and fibrin glue scaffold

Under general anesthesia with a combination of azaperone and tiletamine–zolazepam, the walls of both maxillary sinuses were exposed to an extraoral approach.[12,29] After creating a 1 cm diameter lateral window in the anterior wall of the maxillary sinus, Schneider's membrane was elevated (Fig. 5A). At the experimental sites, 1×10^{7} autogenous SDMSCs labeled with PKH26 were transplanted into the space between Schneider's membrane and the sinus wall with a mixture of 0.25 cm^3 of DMB (Grafton; Osteotech) and 0.3 mL of fibrin glue (Greenplast kit). At the contralateral control site, maxillary sinus floor elevation was performed using only a DMB and fibrin glue scaffold. Finally, the lateral windows of the sinus walls were covered with resorbable bovine collagen dura mater (Lyoplant®; Aesculap, Melsungen, Germany). The wounds were closed in two layers using 3-0 Vicryl for the muscle and 3-0 nylon for the skin. A first-generation cephalosporin (Cefazolin®, 20 mg/kg for 5 days; Yuhan, Seoul, Korea) and an antiinflammatory drug (Meloxicam®, 2 mg/kg for a day; Boehringer Ingerheim, Ingelheim, Germany) were injected intramuscularly twice a day.

Histological analysis of in vivo *osteogenesis*

Under general anesthesia, two animals, each at 2 and 4 weeks after sinus grafting, were euthanized by KCl injection. The maxillary sinus anterior wall, including the grafted area, was harvested *en bloc*, and the specimens were then carefully separated into two sections for histological studies and fluorescent observation.

One of the tissue specimens was fixed in 10% neutral-buffered formalin for 24 h and then decalcified in 5% nitric acid for 3 days. The specimen was embedded in a paraffin block, cut into 4 μm sections, and then mounted on the silane-coated slides to minimize tissue loss during the staining process. The sliced sections were maintained at room temperature for 12 h and then deparaffinized. Hematoxylin and eosin staining was conducted after hydration was accomplished. Immunohistochemical staining for osteocalcin was conducted using an automated immunostainer (LabVision Autostainer™; LabVision, Thermo Fisher Scientific Inc., Fremont, CA). Deparaffinization and antigen retrieval of specimens were performed simultaneously using Tris–EDTA buffer (LabVision). Glass slides were incubated in a PTmodule™ (LabVision) at 100°C for 25 min, washed with Tris-buffered saline (LabVision) twice (3 min each time), and treated with hydrogen peroxide at room temperature for 10 min. A 1:200 dilution of primary mouse monoclonal antibody IgG2a (MA1-5071; Thermo Scientific™, Rockford, IL) was used to observe the osteocalcin expression. The sections were treated with hydrogen peroxide to block endogenous peroxidase activity. The sections were then reacted with

primary antibodies against osteocalcin at room temperature for 40 min, treated with a biotinylated polyvalent secondary antibody solution, incubated with a horseradish peroxidase–conjugated avidin–biotin complex, and treated with 3,3-diaminobenzidine and hydrogen peroxidase. Finally, the nuclei were counterstained with hematoxylin. According to the methods reported in a previous study,[30] the intensity of osteocalcin immunostaining in the cellular components of the newly generated bones was analyzed semiquantitatively by two experienced pathologist, both of whom were blinded to the staining and stage. A minimum of three sections per animal were evaluated at each time point for immnunostaining analysis.

The other specimens were used for observation of PKH26-stained cells. Harvested fresh maxillary sinus tissues were embedded in optimum cutting temperature (OCT) compound (Tissue-Tek®; Sakura Finetechnical Co., Ltd., Tokyo, Japan) in Cryomold. After then they were rapidly refrozen at −23°C and cut into 4 μm sections using Cryocut equipment (LEICA CM3050S; Leica, Wetzlar, Germany). The sections were mounted on the silane-coated glass slides and counterstained with 4′,6-diamidino-2-phenylindole (DAPI; Vectasheid®; Vector Lab, Burlingame, CA). Fluorescent expression was assessed by fluorescence microscopy (BX51; Olympus, Tokyo, Japan) using a fluorescent digital camera (DP72; Olympus). The number of cells expressing DAPI or PKH26 was determined using microscope photography, and the cells viewed were counted and calculated per cm^2. A minimum of three sections per animal were evaluated at each time point for *in vivo* fluorescent cell counting.

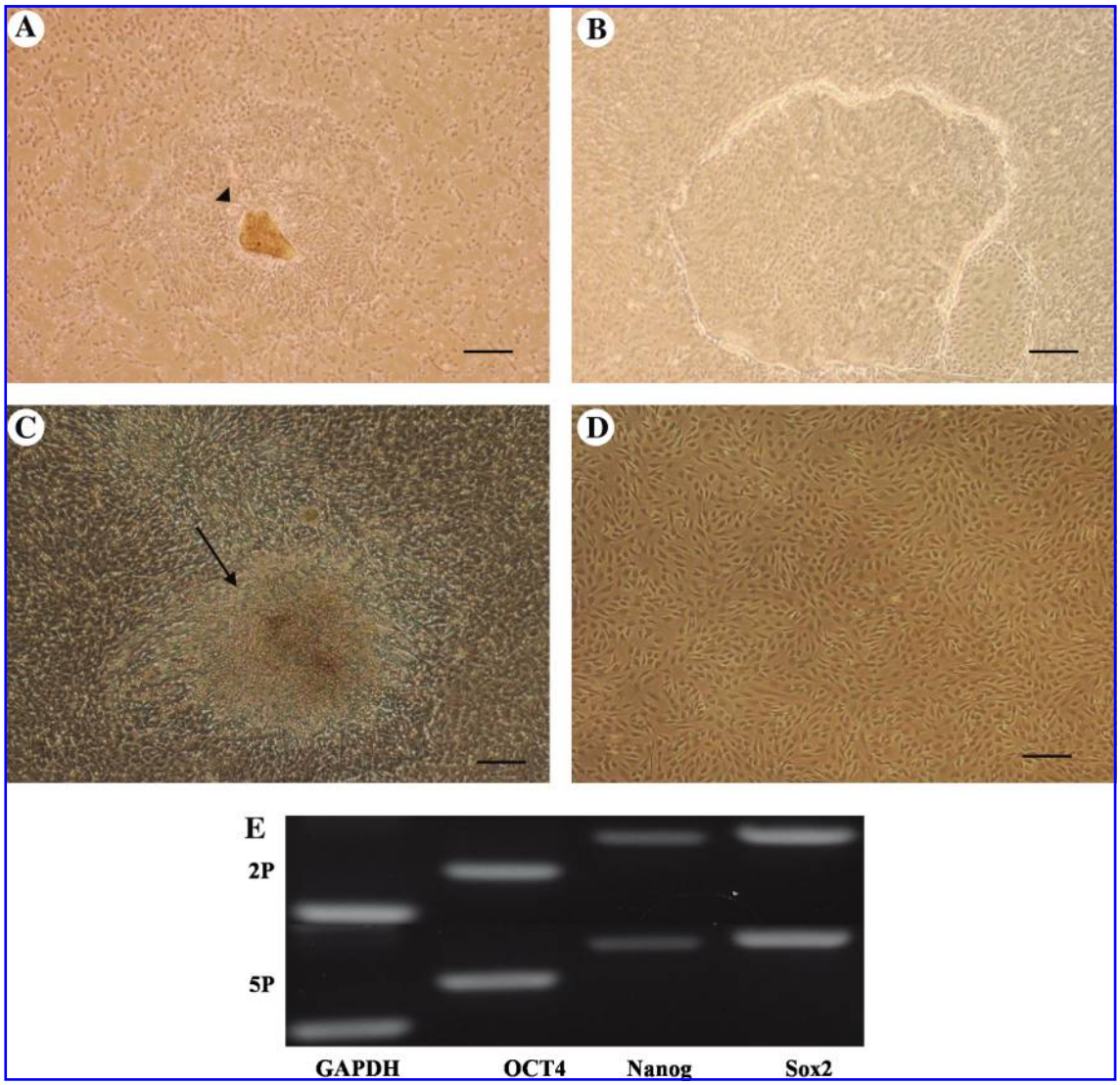

FIG. 1. Isolation and cultivation of skin-derived mesenchymal stem cell–like cells (SDMSCs) from the ear skin of miniature pigs (scale bars = 100 μm). (**A–C**) After 7 days of primary culture (passage 0). (**A**) Unremoved small skin segment (arrowhead) and (**B**) irregular shaped skin-derived cells were observed. (**C**) Colony formation of skin-derived cells (arrow) was also detected in this primary culture period. (**D**) After 3 weeks of culture, homogeneous skin-derived cells were observed in the culture plate. (**E**) Transcription factors, Oct-4, Nanog, and Sox-2, were detected on the second (2P) and fifth (5P) passages of skin-derived cells, as demonstrated by reverse transcription–polymerase chain reaction. GAPDH; glyceraldehyde-3-phosphate dehydrogenase. Color images available online at www.liebertonline.com/ten.

Statistical analysis

All values of the counted and calculated cell number in both *in vitro* and *in vivo* specimens were statistical analyzed by Manova test, and independent grouping variables were compared using the Bonferroni and SPSS software (IBM, Chicago, IL). Data were expressed as mean ± standard deviation. Differences were considered to be significant when $p < 0.05$.

Results

Cell isolation and culture

Small skin segments were cultured in the medium based on DMEM/F12 (1:1) supplemented with FBS, FGF2, EGF, and antibiotics. From day 1 of attachment, floating and sphere-like, skin-derived cells were observed around the attached tissues in the culture medium. After 3 days, almost all the cells were adherent on the gelatin-coated plates. The cultured skin-derived cells revealed various irregular shapes and colony formation during the primary culture period (Fig. 1A, B). In these early culturing periods, various round- and polygon–shaped, skin-derived cells were easily observed and grown, forming colonies till passage 2 (Fig. 1C). After three or four passages of culture, homogeneous adherent skin-derived cells were dominantly observed in the culture dishes (Fig. 1D).

Expressions of transcription factors by PCR and MSC markers by fluorescence-activated cell sorting analysis

In these homogeneous porcine skin-derived cells, expressions of transcription factors, such as Oct-4, Nanog, and Sox-2, were observed by RT-PCR at both time points for passages 2 and 5 (Fig. 1E). In addition, the skin-derived cells of fifth passage were positive for typical MSC markers, CD29, CD44, CD90, and vimentin, by fluorescence-activated cell sorting analysis (Fig. 2). These findings demonstrated that the cells used for the study were SDMSCs, by observation of similar characteristics.

In vitro *coculture of pSDMSCs with a DMB and fibrin glue scaffold*

On the first day of cell seeding in the DMB and fibrin glue scaffold, round and homogeneous cells were observed in the scaffold (Fig. 3A). As the culture time progressed, the number of observable cells increased, and a dark brown matrix formed in the coculturing media (Fig. 3B). Moreover, the formation of bone matrix was demonstrated by von Kossa staining of these cocultured cells at 4 weeks (Fig. 3C). Histological features of *in vitro* cocultured matrix showed many live SDMSCs in the DMB and fibrin glue scaffold at all time points (Fig. 3D). In histological sections, the cell count gradually increased from 4.5 ± 1.73 ($\times 10^4/cm^2$), 9.75 ± 2.63 ($\times 10^4/cm^2$), and 17.75 ± 4.79

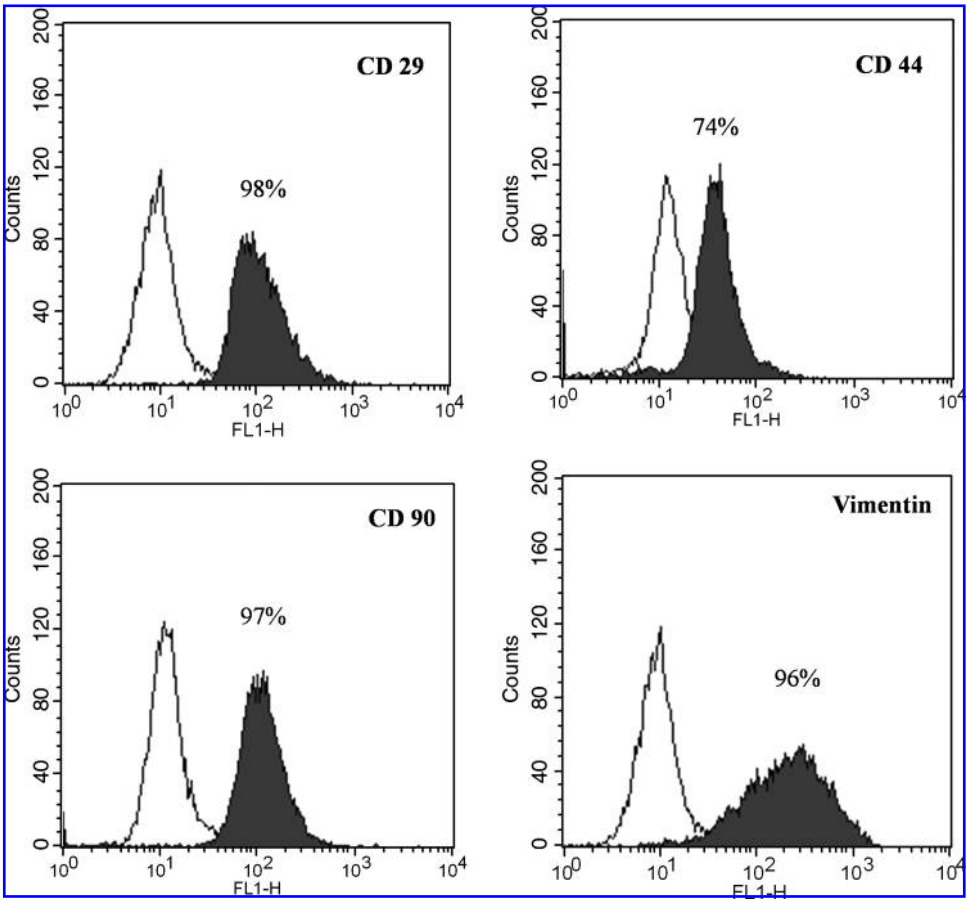

FIG. 2. Fluorescence-activated cell sorting analysis of cultured porcine skin-derived cells. Skin-derived cells of fifth passage were positive for specific MSC markers, CD29, CD44, CD90, and vimentin. Open histograms represent staining with negative control, and the black histograms show the fluorescence intensity of each cell surface antibodies.

($\times 10^4/cm^2$) at 1, 2, and 4 weeks of coculture, respectively, compared with first day of coculture (2.8 ± 0.61 [$\times 10^4/cm^2$]) (Fig. 3E).

The expressions of osteonectin, osteocalcin, and Runx2 in the cocultured cells with the DMB and fibrin glue scaffold at different time points of 1, 2, and 4 weeks were ascertained by RT-PCR (Fig. 4A). Quantitative RT-PCR was used to compare the osteonectin and osteocalcin mRNA levels. The mRNA levels of osteonectin and osteocalcin (1.66 ± 0.13 and 2.13 ± 0.14 at 1 week, 23.43 ± 0.97 and 7.13 ± 1.67 at 2 weeks, and 7.68 ± 0.54 and 3.64 ± 0.35 at 4 weeks, respectively) increased gradually and reached to a maximum at 2 weeks of culture, and then downregulated at 4 weeks of culture (Fig. 4B).

In vivo *osteogenesis of autogenous pSDMSCs in the maxillary sinus floor*

pSDMSCs labeled with PKH26 were found to exhibit red fluorescence under a fluorescent microscope (Fig. 7B). One day after being labeled with PKH26, the pSDMSCs were

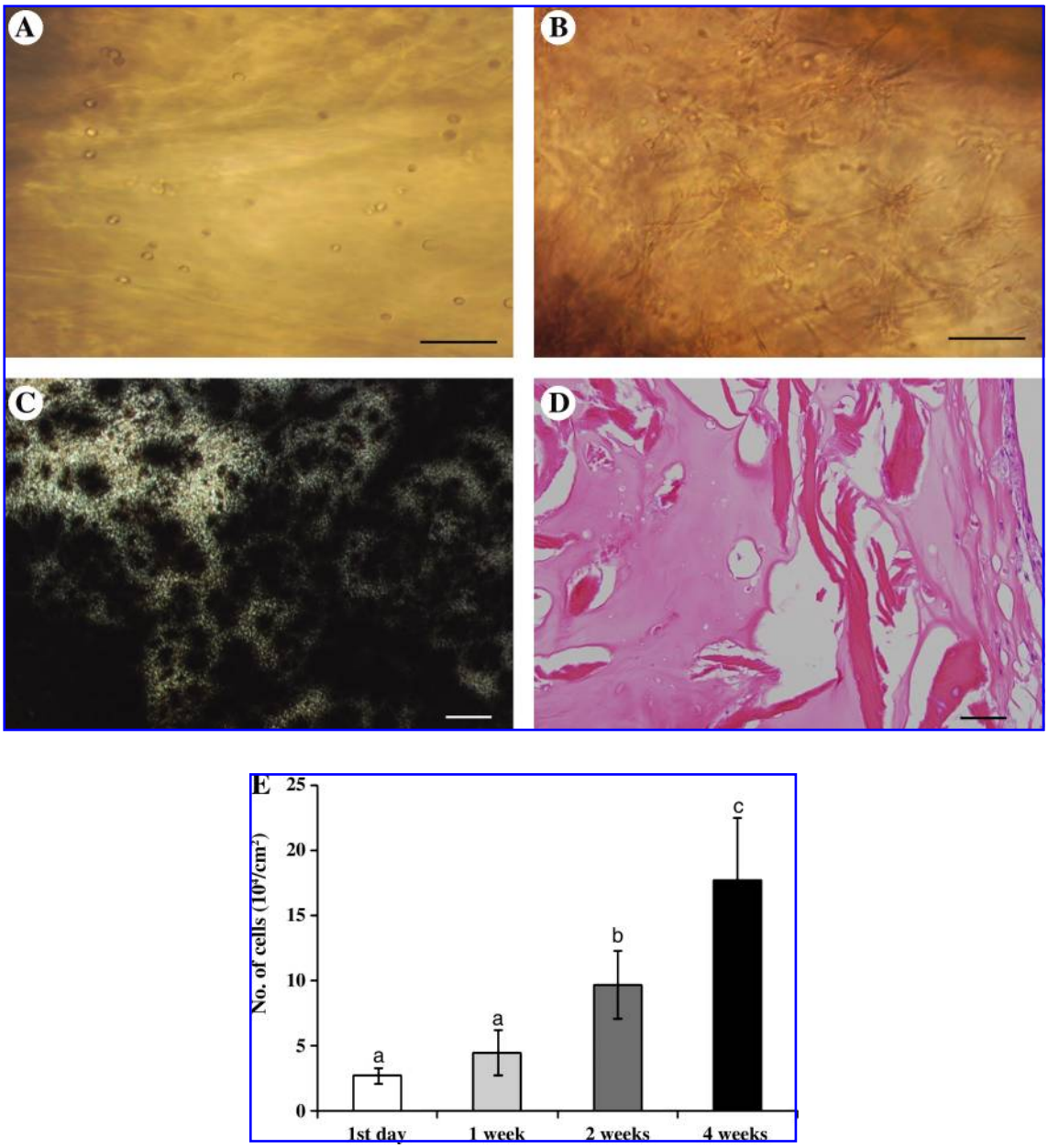

FIG. 3. *In vitro* coculture of SDMSCs with a mixed demineralized bone (DMB) and fibrin glue scaffold in nonosteogenic inductive media. Scale bars: (**A, B**) 100 μm and (**C, D**) 50 μm. (**A**) Round and homogeneous SDMSCs were observed in the mixed scaffold at first day after cell seeding. (**B**) Dark brown matrix and an increased number of cultivated cells were observed at 2 weeks after coculture. (**C**) Enhanced positive von Kossa staining was detected at 4 weeks after *in vitro* coculture. (**D**) On hematoxylin and eosin staining, the seeding cells were well preserved in the scaffold at 4 weeks after *in vitro* coculture. (**E**) The number of *in vitro* cocultured cells increased as time passed. Color images available online at www.liebertonline.com/ten.

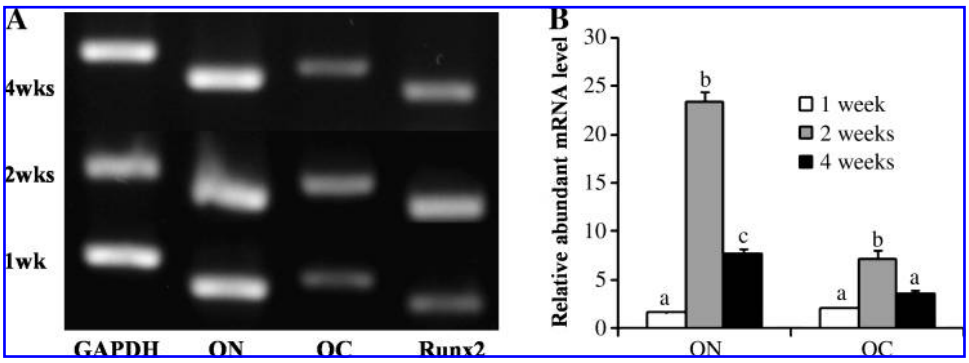

FIG. 4. Reverse transcription–polymerase chain reaction analysis of osteonectin (ON), osteocalcin (OC), and Runx2 in the *in vitro* co-cultured cells with a mixed DMB and fibrin glue scaffold. (**A**) Bands of expressed mRNA appeared on the 1% agarose gel. (**B**) Quantitative comparison of mRNA of the ON and OC in the coculture period. Both ON and OC were most strongly expressed at 2 weeks (Manova test, mean ± standard deviation, $p < 0.05$).

grafted into the maxillary sinus floor with the DMB and fibrin glue scaffold. *In vivo* red fluorescence was observed in the grafted tissues at 2 weeks (Fig. 7D) and at 4 weeks (Fig. 7F) after graft. However, the intensity of fluorescence expression was slightly weakened in the specimen at 4 weeks after graft, compared with the specimen at 2 weeks after graft.

On optical microscopy with hematoxylin and eosin staining, grafted materials were well preserved and formed a sphere shape under Schneider's membrane (Fig. 5B). Two weeks after graft, bone regeneration increased markedly in the experimental specimen compared with the control specimen (Fig. 5C, E). At that time, osteocalcin activity was strongly detected in the experimental specimen, but was hardly observed in the control specimen (Fig. 5D, F). Bone formation and consolidation were significantly enhanced at 4 weeks compared with 2 weeks after graft placement (Fig. 6C). At 4 weeks, osteocalcin activity was also strongly detected in the graft material (Fig. 6D). However, in the control specimens at 4 weeks after graft placement, newly generated bone and osteocalcin were barely observed around the graft material (Fig. 6A, B). The pattern of osteocalcin expression in cellular components of the newly generated trabecular bone is summarized in Table 2. The strongest expression was observed in the immature fibroblast-like cells in the periphery of the graft material at 2 and 4 weeks after *in vivo* grafting (Fig. 6E, F). In contrast to the *in vitro* coculture, the *in vivo* immunohistochemical expression of osteocalcin was slightly stronger in the 4 weeks postgraft specimen compared with the 2 weeks postgraft specimen.

The number of *in vivo* DAPI-stained cells was increased in the 4 weeks' specimen (4.19 ± 0.23 [$\times 10^4/cm^2$]) compared with the 2 weeks' specimen (3.25 ± 0.2 [$\times 10^4/cm^2$]). However, the number of *in vivo* PKH26-expressing cells was decreased in the 4 weeks' specimen (1.44 ± 0.24 [$\times 10^4/cm^2$]) compared with the 2 weeks' specimen (2.93 ± 0.28 [$\times 10^4/cm^2$]) (Fig. 7G).

Discussion

Numerous stem-cell sources have been introduced for application in bone repair, including bone marrow, periosteum, synovium, and skeletal muscle.[31] Moreover, in the interest of successful placement of dental implants in the posterior maxillary ridge, the maxillary sinus floor augmentation has been broadly studied using the tissue-engineered bones. In such studies, the periosteum-derived cells and bone marrow stem cells have been the main sources of tissue-engineered bones. Recently, more easily accessible tissues, such as fat or skin, have been studied as alternative stem-cell sources for tissue-engineered bone. The skin is the largest organ in the body, and it possesses various advantages as a reserve of adult stem cells, including easier acquisition.[13,14,32]

Several characteristics of the skin-derived stem cells have been demonstrated in recent studies, including pluripotency and multilineage differentiation.[15,18,19,32,33] Until now, SKP was most broadly studied in these skin-derived stem cells and isolated from the skins of juvenile and adult rodent,[18,22,23] fetal or adult porcine,[19,20] and neonatal or adult human[13,15,25,32,33]. Originally, SKPs derived from the dermis of skin had the characteristics of embryonic neural crest-derived precursor cells and were isolated under serum-free culturing conditions supplemented with various growth factors, including FGF2, EGF, B27, and/or leukemia inhibitory factor, after enzymatic digestion and dissociation of cells of skin fragments. In the serum-free condition, cultured skin-derived cells formed floating spheres, which were considered as embryonic neural crest-derived SKPs.[21,22,23] However, in the serum-containing medium, the skin-derived cells, which also have multipotency, grew adherently and proliferated into cell clusters.[15,23,32] Recently, Riekstina *et al.*[15] observed the positive MSC markers, such as CD90, CD73, and CD105, in their isolated adherent SKPs under serum-containing condition, and therefore they concluded that their isolated SKPs were skin-derived MSCs (S-MSCs). They also observed that FBS had the most pronounced dose-dependent effect on S-MSC proliferation, and the cocktail of growth factors (EGF, FGF2, B27, and leukemia inhibitory factor) for S-MSC culture could be replaced with FGF2 alone or FGF2 with B27 in the basal culture medium.[15] In this study, we have also successfully isolated and cultured homogeneous skin-derived cells with similar culture conditions and supplementations.

Recently, several characteristics of MSCs were known: first, MSCs are plastic adherent in standard culture conditions; second, they express the cell surface markers CD13, CD29, CD44, CD73, CD90, CD105, and CD166; and third, they differentiate into osteocytes, adipocytes, and chodroblasts *in vitro*.[9,34] Although these CD marker criteria apply only to human MSCs,[34] we detected the positive expression of CD29, CD44, and CD90 in our isolated porcine skin-derived cells using porcine cell surface antibodies. In

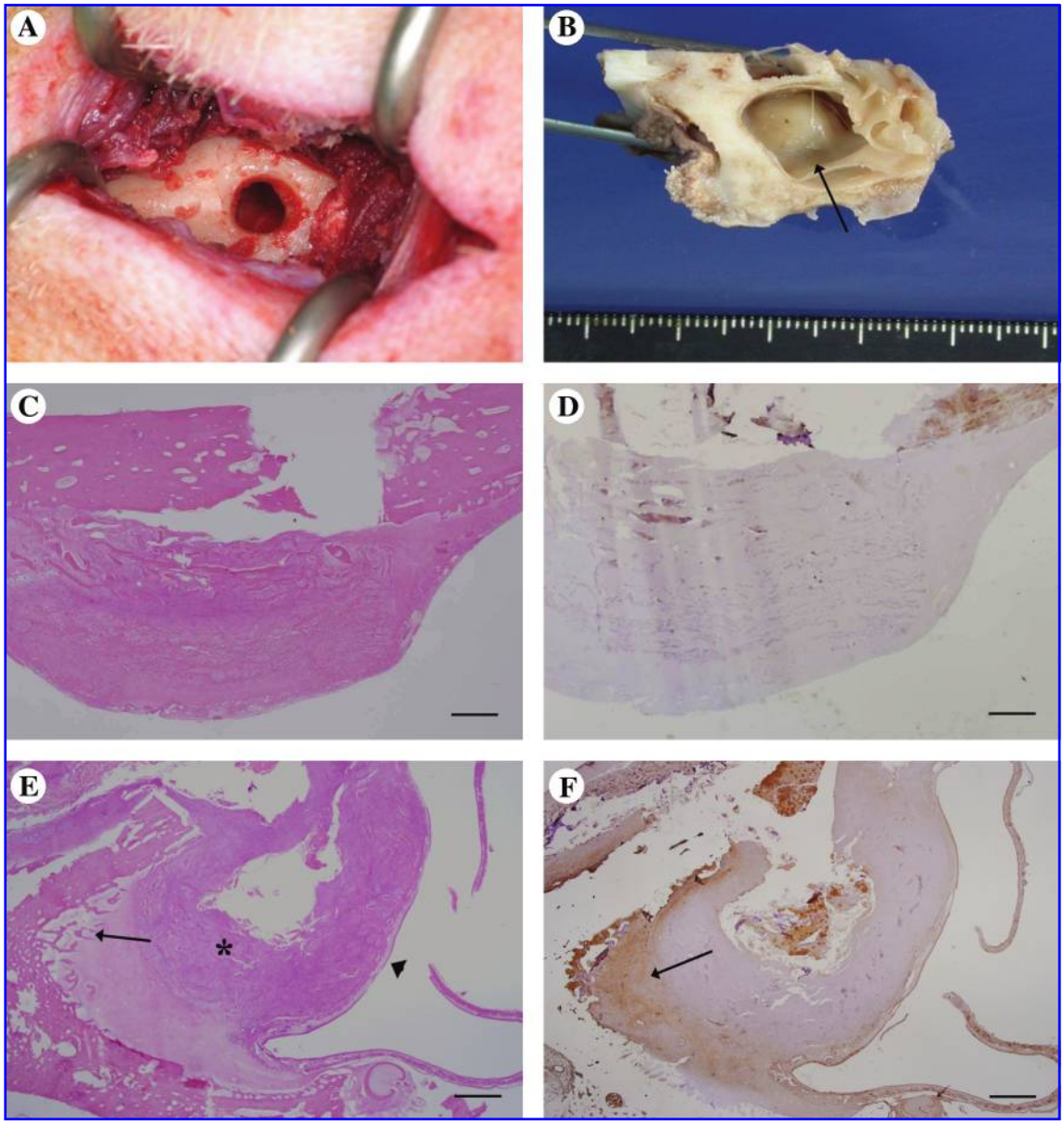

FIG. 5. Maxillary sinus floor elevation using autogenous SDMSCs. (**A**) The lateral window was formed via an extraoral approach in the anterior wall of the maxillary sinus. (**B**) Augmented graft material was found under Schneider's membrane in the harvested specimen (arrow). (**C–F**) Histologic appearances at 2 weeks after maxillary sinus floor elevation (scale bars = 1000 μm). (**C, D**) Control group. Grafted DMB bone matrix was noted, but newly generated bone was not clearly detected in the sinus-grafted material (**C**). Expression of osteocalcin was also nearly negative in the graft material (**D**). (**E, F**) Experimental group. The grafted material (*) was well preserved under Schneider's membrane (arrowhead), and new trabecular bones (arrow) were generated from the periphery of the graft material (**E**). Osteocalcin was strongly expressed in the new bone–generated site of the graft material (arrow) (**F**). Color images available online at www.liebertonline.com/ten.

addition, the cytoskeleton marker of mesenchymal origin, vimentin, was also detected using fluorescence-activated cell sorting analysis (Fig. 2). Our results demonstrated that the cultured skin-derived cells had the characteristic of MSCs. Interestingly, various pluripotency-related genes, including Oct-4,[19,20] Sox-2, and Nanog,[33] were also detected in other studies for skin-derived progenitors. These transcription factors were expressed at high levels in pluripotent cells and were considered markers of primitive stem cells.[35] It was known that these factors were not highly expressed in the postnatal adult stem cells. However, recently after detection of these factors in several postnatal stem cells, such as bone marrow MSCs,[36] adipose-derived stem cells,[37] dental pulp-derived stem cells,[38] umbilical cord matrix cells,[28] and skin-derived stem cells,[19,20,32] the concept was changed. We have also detected the positive expression of Oct-4, Nanog, and Sox-2 in the cultured SDMSCs, at both time points for passages 2 and 5 (Fig. 1E). These results were similar to the previous neurogenic SKP studies.[19,20,32] Moreover, we previously observed the *in vitro* mesodermal and ectodermal

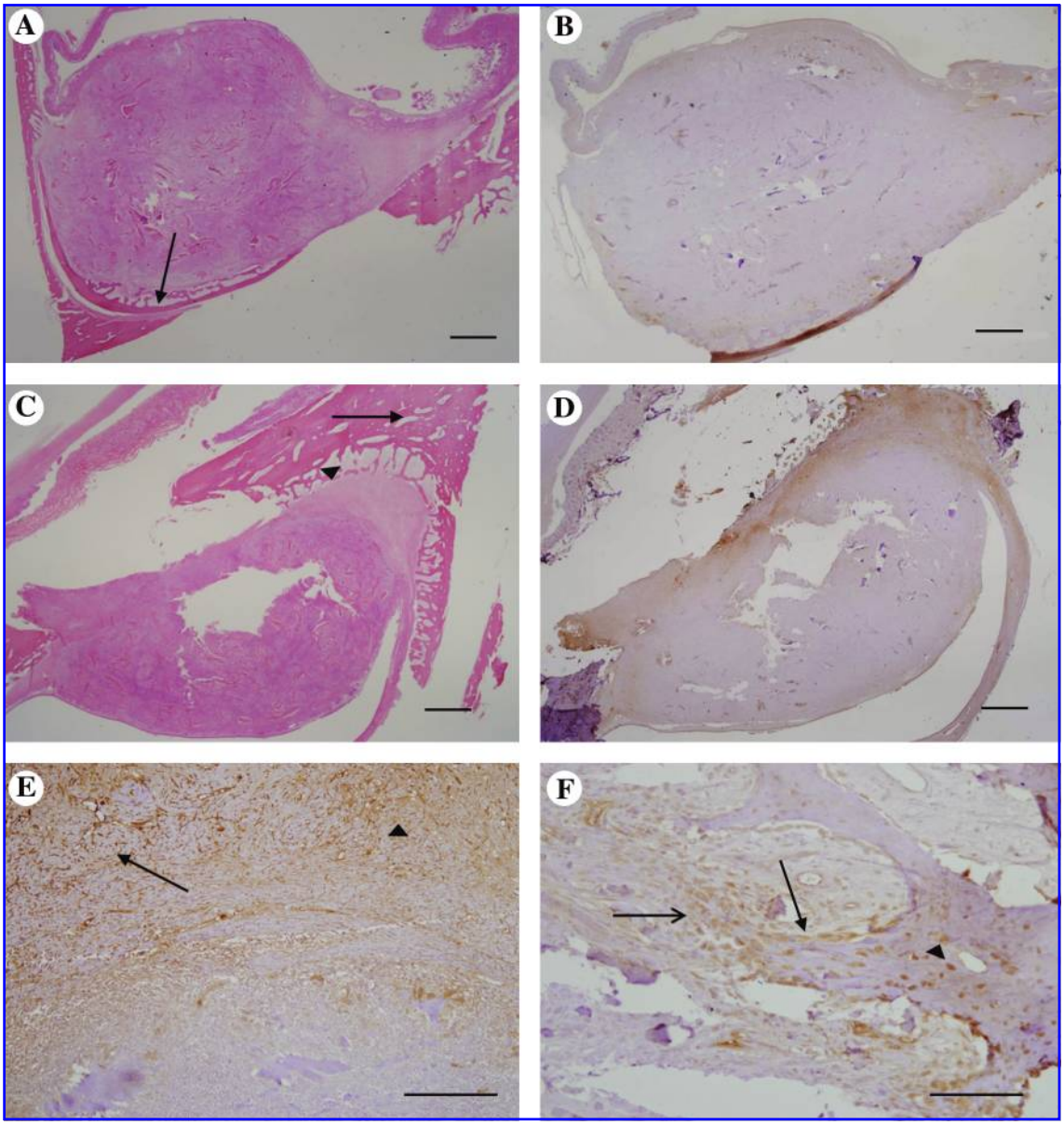

FIG. 6. Histologic features at 4 weeks after maxillary sinus floor elevation. (**A, B**) Control group (scale bars = 1000 μm). Weak new bone activity (arrow) and osteocalcin expression were observed in the periphery of the control specimen. (**C, D**) Experimental group (scale bars = 1000 μm). Enhanced new bone activity (arrowhead) and consolidation of generated bones (arrow) were observed in the grafted tissue (**C**). Strong osteocalcin activity was also observed in these newly generated bone areas (**D**). (**E**) At higher magnification in the experimental specimen, higher bone morphogenic activity (arrow) was observed with enhanced osteocalcin expression in the numerous immature fibroblast-like cells (arrowhead) (scale bar = 200 μm). (**F**) Strong expression of osteocalcin in the immature fibroblast-like cells (→), osteoblasts (➝), and osteocytes (arrowhead) in the newly generated trabecular bone at 4 weeks after graft (scale bar = 100 μm). Color images available online at www.liebertonline.com/ten.

Table 2. Semiquantitative Analysis of *In Vivo* Osteocalcin Staining in Cellular Components of the Newly Generated Bones in the Maxillary Sinus Floor

	Fibroblast-like cells		*Osteoblasts*		*Osteocytes*	
	Control	*Experimental*	*Control*	*Experimental*	*Control*	*Experimental*
2 weeks later	−	+++	−	++	−	++
4 weeks later	+	+++	+	+++	+/−	+++

−, negative expression; +/−, focal or questionable expression; +, weak expression; ++, moderate expression; +++, strong expression.

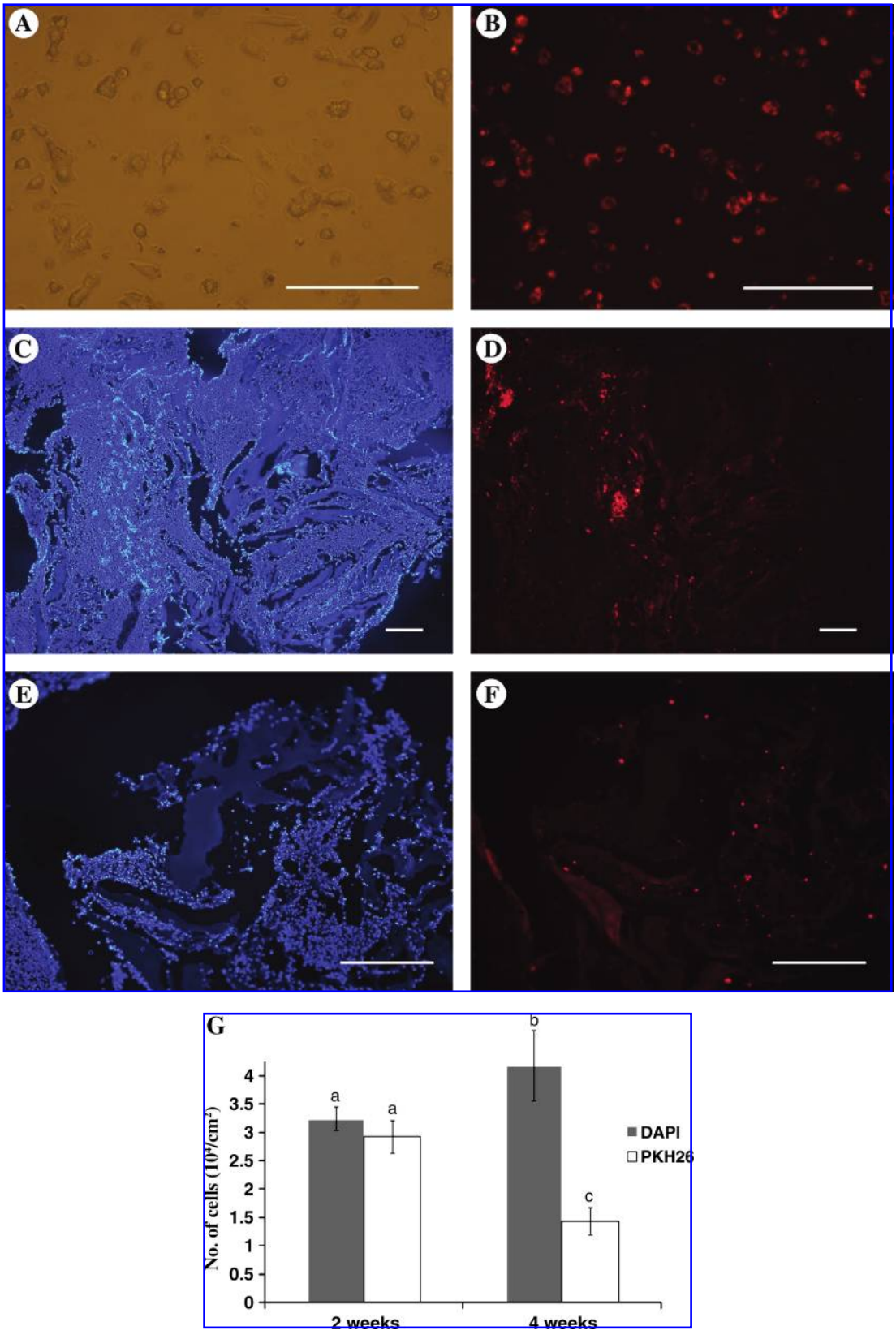

FIG. 7. PKH26 cell labeling and expression in the grafted specimens (scale bars = 100 μm). (**A, B**) Immediately before *in vivo* sinus grafting of autogenous SDSCs. Photomicrographs of SDSCs (**A**) and PKH26 expression (**B**). (**C, D**) Two weeks after *in vivo* sinus graft placement. Numerous nuclei were observed in the grafted material (**C**; 4′,6-diamidino-2-phenylindole [DAPI]), and PKH26-positive cells were also detected in the same specimen (**D**). (**E, F**) Four weeks after *in vivo* graft placement. Abundant cells were observed in the sinus graft material under DAPI staining (**E**). In this period, PKH26 was still detected, but its intensity was weakened (**F**). (**G**) The number of DAPI- and PKH26-stained cells ($10^4/cm^2$) in fresh frozen sections at 2 and 4 weeks after graft placement (Manova test, mean ± standard deviation, $p < 0.05$). Color images available online at www.liebertonline.com/ten.

(osteogenic, adipogenic, and neurogenic) differentiations of skin-derived cells.[27] Based on these data, we presumed that the skin-derived cells of this study were multipotent SDMSCs.

For the *in vivo* application of cultured stem cells, proper scaffold choice is one of the most important elements for developing tissue-engineered bones. Commercially, biodegradable scaffolds have demonstrated favorable results.[1,10,39] However, many researchers have reported that fibrin glue is also an excellent scaffold in tissue engineering because of the initial stability of the grafted stem cells.[5,39,40] In addition, platelet-rich plasma (PRP), which is considered as an autologous fibrin scaffold, has also been used as a scaffold in tissue-engineered bones.[8,41,42] In several studies, the beneficial osteoinductive effect of PRP was doubted.[29,42] However, the the usefulness of PRP and fibrin glue as a cell delivery system has proven advantageous in tissue engineering.[5,7,39,41] In previous studies, fibrin glue was used in combination with DMB,[40] β-tricalcium phosphate,[5] or biosorbable materials[39] for tissue engineering bones. These materials were used specifically to enhance the mechanical stability of grafted materials. In our scaffold combination, fibrin glue was used for the SDMSC delivery system, and DMB was used to enhance the mechanical stability of the scaffold.

Interestingly, in the recent report, dermal fibroblasts could be differentiated into the bone-like tissue in specific induction media *in vitro*.[43] However, in this study, only DMEM with DMB and fibrin glue scaffold was used for *in vitro* differentiation of SDMSCs into bone matrix. In addition, the cultivated cells were well preserved in the mixed scaffold at 1, 2, and 4 weeks after *in vitro* coculture, and the cell number increased during the cultivation period. After 4 weeks of coculture, von Kossa–positive *in vitro* osteogenesis was observed in the nonosteogenic inductive medium (Fig. 3). These results suggest that the SDMSC growth was not disturbed by the DMB and fibrin glue scaffold, but that this scaffold combination enhanced the osteogenic activity of SDMSC. The expressions of osteocalcin, osteonectin, and Runx2 were also detected in all the *in vitro* cocultured cells at all time points with RT-PCR (Fig. 4). Osteonectin and osteocalcin were bone-related glycoproteins secreted by osteoblasts, and Runx2 was the essential protein for osteoblastic differentiation and skeletal morphogenesis during osteogenesis. We hypothesized that the bone morphogenic proteins (BMPs) from DMB might influence SDMSC differentiation into osteogenic cells in spite of culturing in the nonosteogenic inductive medium. It was well known that DMB had BMPs in their compositions, and BMPs could directly induce *in vitro* and *in vivo* osteogenesis.[44–47] Especially, BMP-2 was highly detected in the Grafton matrix, which was used as DMB source in this study, with other growth factors, including insulin-like growth factor-1 and vascular endothelial growth factor.[47] With respect to the quantitative PCR results, osteonectin and osteocalcin peaked at 2 weeks in *in vitro* cocultured cells and decreased at 4 weeks after coculture. This indicates that the peak *in vitro* differentiation of SDMSCs into osteoblasts occurred at 2 or 3 weeks, and osteoblast differentiation from SDMSCs decreased as time passed. This phenomenon might be explained by early aging or osteocyte transference of the differentiated osteoblasts in the *in vitro* culture condition.

In this study, we also observed *in vivo* osteogenesis of SDMSCs with the DMB and fibrin glue scaffold in the maxillary sinus floor. At 2 and 4 weeks after *in vivo* graft placement, enhanced new bone activity was observed in the autogenous SDMSC-grafted sites compared with the non–SDMSC-grafted sites. In the autogenous SDMSC-grafted group, expression of osteocalcin was increased at the periphery of the graft material, and new bone was found to be growing from the periphery (Figs. 5 and 6). Although further long-term *in vivo* studies are required, this result may be related to the blood supply around graft material in the maxillary sinus floor. Alternately, the peripheral portion of graft material might have more abundant blood supply compared with the central portion, and therefore the commencement of *in vivo* osteogensis was observed in the peripheral portion of the grafted material. In contrast to the *in vitro* cocultured result, osteocalcin expression in the *in vivo* specimens was slightly stronger at 4 weeks after graft than it was at 2 weeks after graft. This suggests that the *in vivo*–transplanted autogenous SDMSCs might survive for a long period of time and differentiate into osteoblasts at an ideal time for *in vivo* bone formation. Most strong *in vivo* osteocalcin expression was observed in the immature fibroblast-like cells in the periphery of the graft material, which corroborated to the findings in the study of distraction osteogenesis.[30] In the distraction osteogenesis procedure, numerous immature fibroblast-like cells were observed at an early time, and they were transferred to osteoblasts and osteocytes for generating and consolidating new bones.

The grafted cells were labeled with PKH26 at 1 day before grafting. At 2 and 4 weeks after graft placement, PKH26 was detected in the *in vivo* osteogenesis of the maxillary sinus floor. PKH26 intensity was weakened in the specimens at 4 weeks after graft compared with 2 weeks after graft. However, based on DAPI staining, the total cell number was increased at 4 weeks after graft (Fig. 7G). This might be related to the half-life of PKH26 and the diminishing fluorescent activity as time passed. However, this observation might also be explained by the differentiation of grafted autogenous SDMSCs into other cell types, such as osteogenic cells, and these differentiated cells might also have proliferated in our experimental scaffold conditions. This theory is supported by the enhanced osteocalcin activity in the grafted material of the experimental group at 4 weeks after graft. This indicates that the grafted autogenous SDMSCs differentiated into osteogenic cells and then proliferated in the maxillary sinus floor.

In conclusion, our results suggest that autogenous SDMSCs with a DMB and fibrin glue scaffold may act as an excellent substitute for bone graft material in maxillary sinus augmentation, although further studies are needed to investigate the clinical uses of SDMSCs. Tissue engineering using autogenous SDMSCs would be useful in the replacement of bone grafting techniques, because skin is an easily obtainable autogenous tissue with various primitive or precursor cells.

Acknowledgments

This work was supported by the Korea Research Foundation Grant funded by the Korean Government (KRF-2007-331-E00236 and KRF-2008-313-E00577).

Disclosure Statement

No competing financial interests exist.

References

1. Schmelzeisen, R., Schimming, R., and Sittinger, M. Making bone: implant into tissue-engineered bone for maxillary sinus floor augmentation—a preliminary report. J Craniomaxillofac Surg **31,** 34, 2003.
2. Springer, I.N., Nocini, P.F., Schlegel, K.A., Santis, D.D., Park, J., Warnke, P.H., Terheyden, H., Zimmermann, R., Chiarini, L., Gardner, K., Ferrari, F., and Wiltfang, J. Two techniques for the preparation of cell-scaffold constructs suitable for sinus augmentation: step to clinical application. Tissue Eng **12,** 2649, 2006.
3. Wheeler, S.L., Holmes, R.E., and Calhoun, C.J. Six-year clinical and histologic study of sinus-lift grafts. Int J Oral Maxillofac Implants **11,** 26, 1996.
4. Vacanti, J.P. Beyond transplantation. Arch Surg **123,** 545, 1998.
5. Yamada, Y., Boo, J.S., Ozawa, R., Nagasaka, T., Okazaki, Y., Hata, K., and Ueda, M. Bone regeneration following injection of mesenchymal stem cells and fibrin glue with a biodegradable scaffold. J Craniomaxillofac Surg **31,** 27, 2003.
6. Chen, F., Feng, X., Wu, W., Ouyang, H., Gao, Z., Cheng, X., Hou, R., and Mao, T. Segmental bone tissue engineering by seeding osteoblast precursor cells into titanium mesh-coral composite scaffolds. Int J Oral Maxillofac Surg **36,** 822, 2007.
7. Yamada, Y., Ueda, M., Naiki, T., and Nagasaka, T. Tissue-engineered injectable bone regeneration for osseointegrated dental implants. Clin Oral Implants Res **15,** 589, 2004.
8. Yamada, Y., Nakamura, S., Ito, K., Kohgo, T., Hibi, H., Nagasaka, T., and Ueda, M. Injectable tissue-engineered bone using autogenous bone marrow-derived stromal cells for maxillary sinus augmentation: clinical application report from a 2–6-year follow-up. Tissue Eng A **14,** 1699, 2008.
9. Park, B.W., Hah, Y.S., Kim, D.Y., Kim, J.R., and Byun, J.H. Osteogenic phenotypes and mineralization of cultured human periosteal-derived cells. Arch Oral Biol **52,** 983, 2007.
10. Schimming, R., and Schmelzeisen, R. Tissue-engineered bone for maxillary sinus augmentation. J Oral Maxillofac Surg **62,** 724, 2004.
11. Zizelmann, C., Schoen, R., Metzger, M.C., Schmelzeisen, R., Schramm, A., Dott, B., Bormann, K., and Gellrich, N.C. Bone formation after sinus augmentation with engineered bone. Clin Oral Implants Res **18,** 69, 2007.
12. Fuerst, G., Tangl, S., Gruber, R., Gahleitner, A., Sanroman, F., and Watzek, G. Bone formation following sinus grafting with autogenous bone-derived cells and bovine bone mineral in minipigs: preliminary findings. Clin Oral Implants Res **15,** 733, 2004.
13. Buranasinsup, S., Sila-asna, M., Bunyaratvej, N., and Bunyaratvej, A. *In vitro* osteogenesis from skin-derived precursor cells. Dev Growth Differ **48,** 263, 2006.
14. Shi, C., Zhu, Y., Su, Y., and Cheng, T. Stem cells and their applications in skin-cell therapy. Trends Biotechnol **24,** 48, 2006.
15. Riekstina, U., Muceniece, R., Cakstina, I., Muiznieks, I., and Ancans, J. Characterization of human skin-derived mesenchymal stem cell proliferation rate in different growth conditions. Cytotechnology **58,** 153, 2008.
16. Blanpain, C., and Fuchs, E. Epidermal stem cells of skin. Annu Rev Cell Dev Biol **22,** 339, 2006.
17. Ohyama, M., Terunuma, A., Tock, C.L., Radonovich, M.F., Pise-Masison, C.A., Hopping, S.B., Brady, J.N., Udey, M.C., and Vogel, J.C. Characterization and isolation of stem cell-enriched human hair follicle bulge cells. J Clin Invest **116,** 249, 2006.
18. Toma, J.G., Akhavan, M., Fernandes, K.J., Barnabe-Heider, F., Sadikot, A., Kaplan, D.R., and Miller, F.D. Isolation of multipotent adult stem cells from the dermis of mammalian skin. Nat Cell Biol **3,** 778, 2001.
19. Dyce, P.W., Zhu, H., Craig, J., and Li, J. Stem cells with multilineage potential derive from porcine skin. Biochem Biophys Res Commun **316,** 651, 2004.
20. Zhao, M., Isom, S.C., Lin, H., Hao, Y., Zhang, Y., Zhao, J., Whyte, J.J., Dobbs, K.B., and Prather, R.S. Tracing the stemness of porcine skin-derived progenitors (pSKP) back to specific marker gene expression. Cloning Stem Cells **11,** 111, 2009.
21. Fernandes, K.J., Toma, J.G., and Miller, F.D. Multipotent skin-derived precursors: adult neural crest-related precursors with therapeutic potential. Philos Trans R Soc Lond B Biol Sci **363,** 185, 2008.
22. Fernandes, K.J., Mckenzie, I.A., Mill, P., Smith, K.M., Akhavan, M., Barnabe-heider, F., Biernaskie, J., Junek, A., Kobayashi, N.R., Toma, J.G., Kaplan, D.R., Labosky, P.A., Rafuse, V., Hui, C.C., and Miller, F.D. A dermal niche for multipotent adult-derive precursor cell. Nat Cell Biol **6,** 1082, 2004.
23. Fernandes, K.J., Kobayashi, N.R., Gallagher, C.J., Barnabe-Heider, F., Aumont, A., Kaplan, D.R., and Miller, F.D. Analysis of the neurogenic potential of multipotent skin-derived precursors. Exp Neurol **201,** 32, 2006.
24. Hunt, D.P., Morris, P.N., Sterling, J., Anderson, J.A., Joannides, A., Jahoda, C., Compston, A., and Chandran, S. A highly enriched niche of precursor cells with neuronal and glial potential within the hair follicle dermal papilla of adult skin. Stem Cells **26,** 163, 2008.
25. Shih, D.T., Lee, D.C., Chen, S.C., Tsai, R.Y., Huang, C.T., Tsai, C.C., Shen, E.Y., and Chiu, W.T. Isolation and characterization of neurogenic mesenchymal stem cells in human scalp tissue. Stem Cells **23,** 1012, 2005.
26. Marchesi, C., Pluderi, M., Colleoni, F., Belicchi, M., Meregalli, M., Farini, A., Parolini, D., Draghi, L., Fruguglietti, M.E., Gavina, M., Porretti, L., Cattaneo, A., Battistelli, M., Prelle, A., Moggio, M., Borsa, S., Bello, L., Spagnoli, D., Gaini, S.M., Tanzi, M.C., Bresolin, N., Grimoldi, N., and Torrente, Y. Skin-derived stem cells transplanted into resorbable guides provide functional nerve regeneration after sciatic nerve resection. Glia **55,** 425, 2007.
27. Choi, M.J., Byun, J.H., Kang, E.J., Rho, G.J., Kim, U.K., Kim, J.R., and Park, B.W. Isolation of porcine multipotential skin-derived precursor cells and its multilineage differentiation. J Kor Oral Maxillofac Surg **34,** 588, 2008.
28. Carlin, R., Davis, D., Weiss, M., Schultz, B., and Troyer, D. Expression of early transcription factors Oct-4, Sox-2 and Nanog by porcine umbilical cord (PUC) matrix cells. Reprod Biol Endocrinol **4,** 8, 2006.
29. Fürst, G., Gruber, R., Tangl, S., Zechner, W., Haas, R., Mailath, G., Sanroman, F., and Watzek, G. Sinus grafting with autogenous platelet-rich plasma and bovine hydroxyapatite. A histomorphometric study in minipigs. Clin Oral Implants Res **14,** 500, 2003.
30. Byun, J.H., Park, B.W., Kim, J.R., and Lee, J.H. Expression of vascular endothelial growth factor and its receptors after mandibular distraction osteogenesis. Int J Oral Maxillofac Surg **36,** 338, 2007.
31. Waese, E.Y., Kandel, R.R., and Stanford, W.L. Application of stem cells in bone repair. Skeletal Radiol **37,** 601, 2008.

32. Kajahn, J., Gorjup, E., Tiede, S., von Briesen, H., Paus, R., Kruse, C., and Danner, S. Skin-derived human adult stem cells surprisingly share many features with human pancreatic stem cells. Eur J Cell Biol **87,** 39, 2008.
33. Toma, J.G., McKenzie, I.A., Bagli, D., and Miller, F.D. Isolation and characterization of multipotent skin-derived precursors from human skin. Stem Cells **23,** 727, 2005.
34. Rho, G.J., Kumar, B.M., and Balasubramanian, S. Porcine mesenchymal stem cells—current technological status and future perspective. Front Biosci **14,** 3942, 2009.
35. Boyer, L.A., Lee, T.I., Cole, M.F., Johnstone, S.E., Levine, S.S., Zucker, J.P., Guenther, M.G., Kumar, R.M., Murray, J.L., Jenner, R.G., Gifford, D.K., Melton, D.A., Jaenisch, R., and Young, R.A. Core transcriptional regulatory circuitry in human embryonic stem cells. Cell **122,** 947, 2005.
36. Izadpanah, R., Joswig, T., Tsien, F., Dufour, J., Kirijan, J.C., and Bunnell, B.A. Characterization of multipotent mesenchymal stem cells from the bone marrow of rhesus macaques. Stem Cells Dev **14,** 440, 2005.
37. Zhu, Y., Liu, T., Song, K., Fan, X., Ma, X., and Cui, Z. Adipose-derived stem cell: a better stem cell than BMSC. Cell Biochem Funct **26,** 664, 2008.
38. Cheng, P.H., Snyder, B., Fillos, D., Ibeqbu, C.C., Huang, A.H., and Chan, A.W. Postnatal stem/progenitor cells derives from the dental pulp of adult chimpanzee. BMC Cell Biol **9,** 20, 2008.
39. Perka, C., Schultz, O., Spitzer, R.S., Lindenhayn, K., Burmester, G.R., and Sittinger, M. Segmental bone repair by tissue-engineered periosteal cell transplants with biosorbable fleece and fibrin scaffolds in rabbits. Biomaterials **21,** 1145, 2000.
40. Schwarz, N., Redl, H., Schlag, G., Schiesser, A., Lintner, F., Dinges, H.P., and Thurnher, M. The influence of fibrin sealant on demineralized bone matrix-dependent osteoinduction. A quantitative and qualitative study in rats. Clin Orthop Relat Res **238,** 282, 1989.
41. Pieri, F., Lucarelli, E., Corinaldesi, G., Fini, M., Aldini, N., Giardino, R., Donati, D., and Marchetti, C. Effect of mesenchymal stem cells and platelet-rich plasma on the healing of standardized bone defects in the alveolar ridge: a comparative histomorphometric study in minipigs. J Oral Maxillofac Surg **67,** 265, 2009.
42. Klongnoi, B., Rupprecht, S., Kessler, P., Thorwarth, M., Wiltfang, J., and Schlegel, K.A. Influence of platelet-rich plasma on a bioglass and autogenous bone in sinus augmentation. An explorative study. Clin Oral Implants Res **17,** 312, 2006.
43. Sommar, P., Pettersson, S., Ness, C., Johnson, H., Kratz, G., and Junker, J.P.E. Engineering three-dimensional cartilage- and bone-like tissues using human dermal fibroblasts and macroporous gelatine microcarriers. J Plast Reconstr Aesthet Surg DOI:10.1016/j.bjps.2009.02.072, 2009 Mar 28. [Epub ahead of print].
44. Buser, D., Hoffmann, B., Bernard, J.P., Lussi, A., Mettler, D., and Schenk, R.K. Evaluation of filling materials in membrane-protected bone defects. A comparative histomorphometric study in the mandible of miniature pigs. Clin Oral Implants Res **9,** 137, 1998.
45. Jeon, O., Rhie, J.W., Kwon, I.K., Kim, J.H., Kim, B.S., and Lee, S.H. *In vivo* bone formation following transplantation of human adipose-derived stromal cells that are not differentiated osteogenically. Tissue Eng A **14,** 1285, 2008.
46. Hasegawa, Y., Shimasa, K., Suzuki, N., Takayama, T., Kato, T., Iizuka, T., Sato, S., and Ito, K. The *in vitro* osteogenetic characteristics of primary osteoblastic cells from a rabbit calvarium. J Oral Sci **50,** 427, 2008.
47. Wildemann, B., Kadow-Romacker, A., Haas, N.P., and Schmidmaier, G. Quantifications of various growth factors in different demineralized bone matrix preparations. J Biomed Mater Res **81A**, 437, 2007.

Address correspondence to:
Bong-Wook Park, D.D.S., Ph.D.
Department of Oral & Maxillofacial Surgery
School of Medicine and Institute of Health Sciences
Gyeongsang National University
Chilam-dong 90
Jinju
Gyeongnam 660-702
Republic of Korea

E-mail: parkbw@gsnu.ac.kr

Received: June 30, 2009
Accepted: September 23, 2009
Online Publication Date: November 11, 2009